Supporting Information

Xin et al. 10.1073/pnas.1313192110

SI Materials and Methods

Generation of αMHC-YapS112A Transgenic Mice. Transgenic (Tg) mice were generated by pronuclear injection according to standard procedures. A full-length mouse cDNA encoding YapS112A with a Flag epitope tag was cloned 3′ to a 5.5-kb segment of the α-myosin heavy chain promoter (αMHC) and 5′ to a 0.6-kb polyadenylation signal from the human growth hormone gene. The transgene was linearized with NotI, to remove vector sequence, injected into fertilized oocytes from B6C3F1 female mice, and implanted into pseudopregnant ICR mice.

Creation of a Conditional *Taz* Mutant Allele. The Taz targeting vector was constructed using pGKneoF2L2DTA harboring two loxP sites encompassing a neomycin resistance cassette flanked by two FRT sites. Targeting arm sequences were isolated from 129SvEv genomic DNA by PCR. The Taz 5′ targeting arm (5 kb), Taz 3′ targeting arm (4 kb), and Taz knockout arm (2 kb) were cloned into the vector using EcoRV, EcoRV, and XmaI, respectively. The sequence-verified targeting vector was linearized and electroporated into 129SvEv-derived ES cells. Targeting of the mutant allele was screened through Southern blot analysis. The *Taz* 5′ probe detected a 10-kb fragment in addition to the WT 12-kb fragment on StuI digestion, and the *Taz* 3′ probe detected an 8-kb fragment in addition to the WT 10-kb fragment on BamHI digestion when homologous recombination occurred.

Targeted ES cells were injected into blastocysts to generate chimeric mice. High-percentage chimeric males were bred with mice expressing FLPe recombinase to remove the neomycin resistance cassette to generate Taz^{loxP} alleles (46). PCR genotyping using a forward primer upstream of the 5′ loxP site, a first reverse primer located in the knockout arm, and a second reverse primer downstream of the 3′ loxP site produced a 655-bp band for Taz^{loxP}, a 496-bp band for for Taz^{WT}, and a 704-bp band for Taz^{floxed} alleles. Primer sequences for PCR genotyping were as follows:

TF: 5′GGCTTGTGACAAAGAACCTGGGGCTATCTGAG

TR1: CCCACAGTTAAATGCTTCTCCCAAGACTGGG

TR2: AACTGCTAACGTCTCCTGCCCCTGACCTCTC.

All animal experimental procedures were reviewed and approved by the Institutional Animal Care and Use Committees of the University of Texas Southwestern Medical Center.

Histology and Immunostaining. Hearts were fixed in 4% paraformaldehyde in PBS, embedded in paraffin, and sectioned at 5-μm intervals. H&E staining and Masson's trichrome staining were performed following standard procedures. For immunostaining, slides were deparaffinized and rehydrated, and washed in PBS three times, followed by permeabilization in PBS/0.3% Triton for 10 min and blocking in PBS/5% normal horse serum for 1 h at room temperature. Sections were incubated with specific antibodies overnight at 4 °C. After washing with PBS, the sections were incubated with the secondary antibody for 2 h at room temperature, then washed and sealed with a mounting medium containing DAPI (Vector Laboratories). A similar protocol was used for staining with biotin-labeled lectin *Bandeiraea simplicifolia* (1:200; Vector Laboratories), except that Texas red-conjugated streptavidin (1:200; Vector Laboratories) was used after the biotinylated lectin. Antibodies used in this study include rabbit anti-PH3 (1:200; Cell Signaling), Cy3 conjugated mouse anti–smooth muscle α-actin (1:00; Sigma-Aldrich), and mouse anti- cardiac troponin T (cTnT, 1:400; Thermo Scientific).

Western Blot Analysis. Total heart lysate was prepared by homogenizing frozen tissue in RIPA buffer (50 mM Tris, 150 mM NaCl, 0.1% SDS, 0.5% sodium deoxycholate, 1% Nonidet P-40, and protease inhibitor mixture; Roche). Total cell lysates from neonatal rat cardiomyocytes were prepared by lysing the cells with RIPA buffer. Lysates were then resolved by SDS/PAGE and analyzed to detect proteins of interest. The following antibodies were used: rabbit anti-Yap (1:1,000; Cell Signaling), rabbit anti–phospho-Yap (1:1,000; Cell Signaling), rabbit anti-Igf1r (1:1,000; Cell Signaling), rabbit anti-Akt (1:1,000; Cell Signaling), and rabbit anti–phospho-Akt (1:1,000; Cell Signaling). Anti-rabbit HRP or anti-mouse HRP (1:5,000; Bio-Rad) was used as a secondary antibody, followed by detection with an ECL detection kit (Amersham).

Transthoracic Echocardiography. Cardiac function and heart dimensions were evaluated by 2D echocardiography on conscious mice. M-mode tracings were used to measure anterior and posterior wall thicknesses at end diastole and end systole. Left ventricular (LV) internal diameter (LVID) was measured as the largest anteroposterior diameter in diastole (LVIDd) or systole (LVIDs). A single observer blinded to mouse genotypes analyzed all data. LV fractional shortening (FS) was calculated according to the following formula: $FS\ (\%) = [(LVIDd - LVIDs)/LVIDd] \times 100$.

RNA Analysis. Total RNA was purified from isolated heart ventricles with TRIzol reagent (Invitrogen) according to the manufacturer's instructions. cDNA was synthesized using random hexamers with 2 μg of RNA as a template. Quantitative real-time PCR (qPCR) was performed using an ABI 7000 cycler or a 7900HT cycler (Applied Biosystems). PCR reactions were amplified with gene-specific primers in TaqMan buffers (Applied Biosystems) under the following PCR cycle conditions: 95 °C for 3 min, followed by 40 cycles of 95 °C for 30 s and 60 °C for 30 s. The copy number value was calculated from a standard curve generated using a series of diluted plasmids as a template. Gapdh was used for normalization of gene expression in qPCR.

Neonatal Myocardial Infarction. Neonates were anesthetized by cooling on an ice bed. Lateral thoracotomy at the fourth intercostal space was performed by blunt dissection of the intercostal muscles after skin incision. A tapered needle (C-1) attached to a 6–0 prolene suture (Ethicon; Johnson & Johnson) was passed through the midventricle below the origin of the left anterior descending coronary artery (LAD) and tied to induce myocardial infarction (MI). The pericardial membrane remained intact after LAD ligation. Myocardial ischemia was indicated by the light pallor of the myocardium below the ligature after suturing. After LAD ligation, neonates were removed from the ice bed, thoracic wall incisions were sutured with a 6–0 nonabsorbable prolene suture, and the skin wound was closed by using skin adhesive. Sham-operated mice underwent the same procedure involving hypothermic anesthesia and thoracotomy without LAD ligation. No differences in myocyte proliferative response were observed between sham-operated mice (hypothermic anesthesia and thoracotomy) and unoperated control mice. After surgery, neonates were warmed for several minutes under a heating lamp until recovery. The entire procedure lasted ∼10 min.

The vast majority (90%) of the sham-operated and LAD-ligated postnatal day (P) 1 and P7 neonates survived the surgical procedure, with all deaths occurring during or on the day of surgery; however, maternal cannibalization reduced survival rates

in the MI group to ~70% by the next day. For MI surgeries at P14, mice were anesthetized with isoflurane, followed by endotracheal intubation for ventilation using a small animal ventilator (Harvard Apparatus).

Adult MI. Adult mice were anesthetized with isoflurane, intubated with a polyethylene tube (size 60), and then ventilated with a volume-cycled rodent respirator with 2–3 mL per cycle at a respiratory rate of 120 cycles/min. Thoracotomy was performed at the third intercostal space, and self-retaining microretractors were placed to separate the third and fourth rib to visualize the LAD. A 7.0 prolene suture (Ethicon, Johnson & Johnson) was then passed under the LAD at 1.5 mm distal to the left atrial appendage, immediately after the bifurcation of the left main coronary artery. The LAD was doubly ligated. The occlusion was confirmed by the change in color (becoming paler) of the anterior wall of the left ventricle. Sham-operated mice underwent the same procedure without ligation.

Triphenyltetrazolium Chloride Staining. The excised hearts were perfused with Krebs–Henseleit solution using a Langendorff apparatus. To delineate infarcted from viable myocardium, the hearts were perfused with a 1% solution of triphenyltetrazolium chloride (TTC) in phosphate buffer (pH 7.4) at 37 °C at a pressure of 60 mmHg (~5 mL over 5 min). The hearts were frozen, then cut into six transverse slices, which were fixed in 10% neutral buffered formaldehyde and photographed.

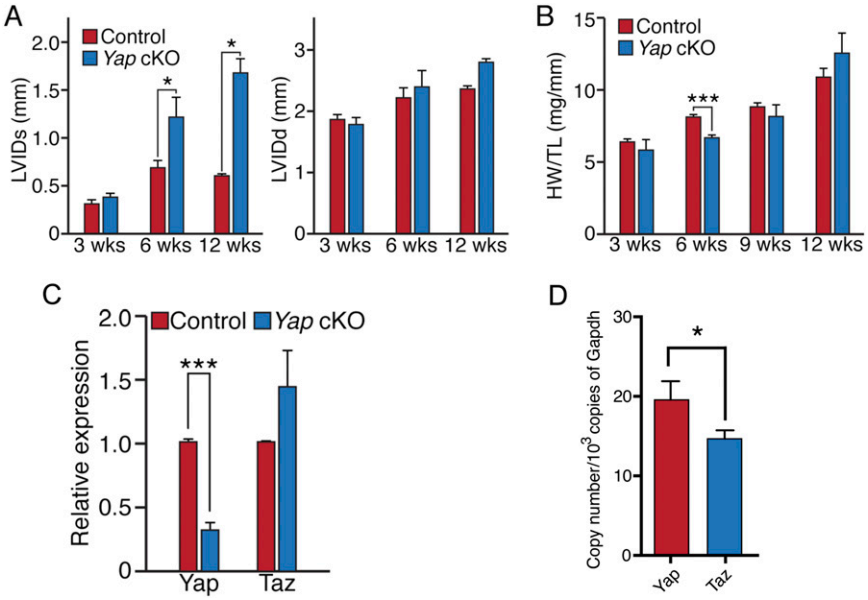

Fig. S1. Analyses of Yap cKO and WT mice. (*A*) Yap mutant mice display abnormal LV dilation during systole and diastole compared with control mice. (*B*) Measurement of the ratio of heart weight (HW) to tibia length (TL) at different time points. (*C*) qPCR analysis demonstrating deletion of Yap in cardiomyocytes. RNA was isolated from the left ventricle of 6-wk-old male mice. Control and Yap cKO indicate $Yap^{loxP/loxP}$ and $Yap^{loxP/loxP}$; αMHC-Cre, respectively. (*D*) qPCR performed using RNA isolated from adult cardiomyocytes. Relative expression was normalized to GAPDH. $n = 3$. Data are mean ± SD. $^{*}P < 0.05$; $^{***}P < 0.001$.

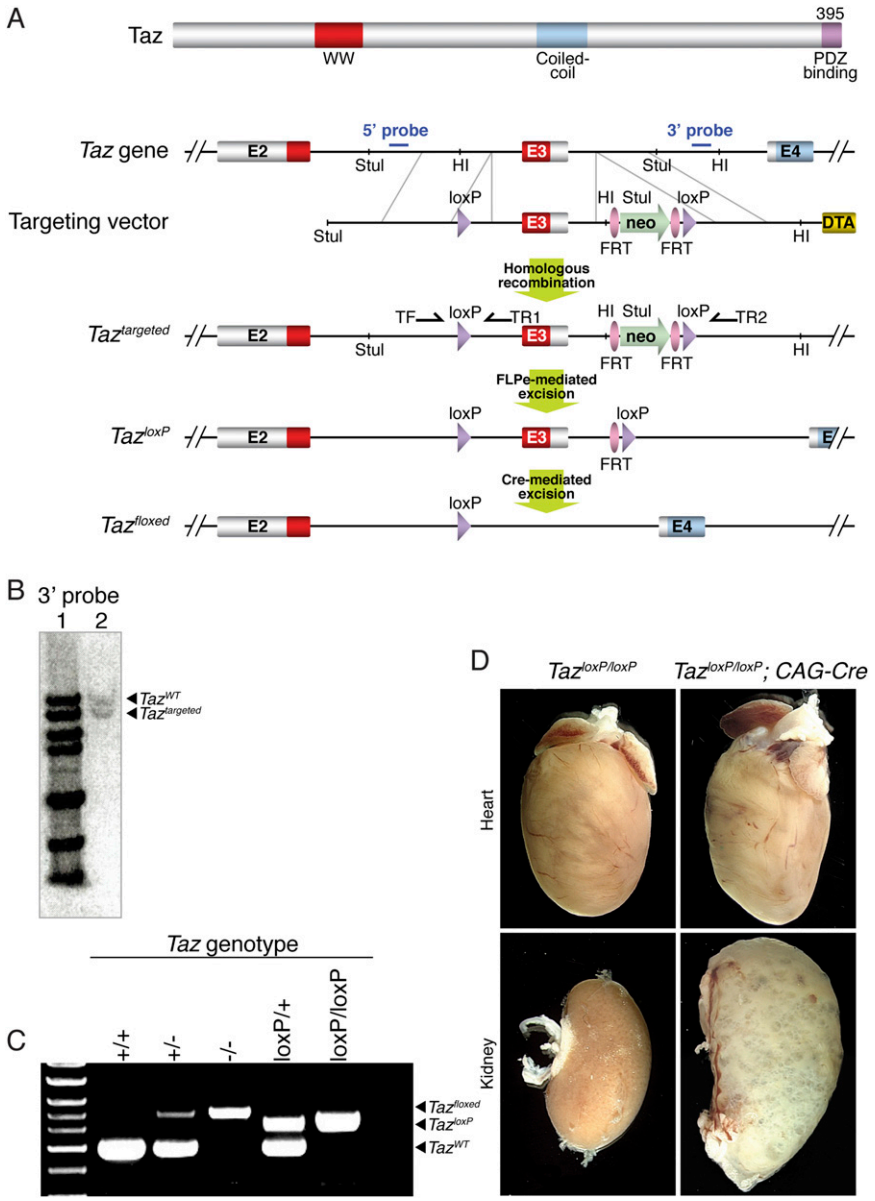

Fig. S2. Generation of mice with a conditional Taz mutant allele. (*A*) Schematic representation of the mouse Taz locus and the targeting strategy. Positions of Southern blot probes and locations of restriction enzyme sites are indicated. Homologous recombination in ES cells and recombinase-mediated excisions generated the Taz^{floxed} allele, in which exon 3 is replaced by one loxP site. Genotyping primers are designated TF, TR1, and TR2. DTA, diptheria toxin A; E, exon; FRT, FLP recombinase target; HI, BamHI; neo, neomycin resistance cassette. (*B*) Southern blot analysis. (*1*) Size markers. (*2*) DNA isolated from Taz$^{targeted/+}$ mice, probed with a 3′ arm probe. Two DNA fragments of 9.5 kb (Taz^{WT}) and 6.2 kb (Taz^{targeted}) are shown, indicating successful homologous recombination at the mouse Taz locus. (*C*) PCR genotyping performed to distinguish different Taz alleles and to confirm excision of Taz exon 3. (*D*) Mice lacking Taz globally that were generated using CAG-Cre were found to suffer from polycystic kidney disease, confirming the previously reported phenotype of Taz null mice (1).

1. Makita R, et al. (2008) Multiple renal cysts, urinary concentration defects, and pulmonary emphysematous changes in mice lacking TAZ. *Am J Physiol Renal Physiol* 294(3):F542–F553.

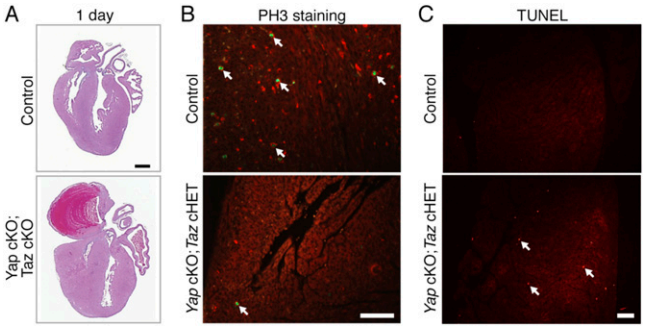

Fig. S3. Compound Yap and Taz mutants exhibit cardiac abnormalities and defects in proliferation and survival. (*A*) H&E-stained heart sections from control ($Yap^{fl/fl}$: $Taz^{fl/fl}$) and Yap cKO; Taz cKO mice at P1. (Scale bar: 1 mm) (*B*) PH3-stained sections of hearts from control ($Yap^{fl/fl}$: $Taz^{fl/+}$) and Yap cKO; Taz cHET mice at P1. The green signal and white arrows indicate PH3-positive staining, and the red signal indicates cTnT immunostaining. (Scale bar: 200 μm.) (*C*) TUNEL-stained sections of hearts from control ($Yap^{fl/fl}$; $Taz^{fl/+}$) and Yap cKO; Taz cHET mice at P4. The red signal and white arrows indicate TUNEL-positive staining. (Scale bar: 200 μm.)

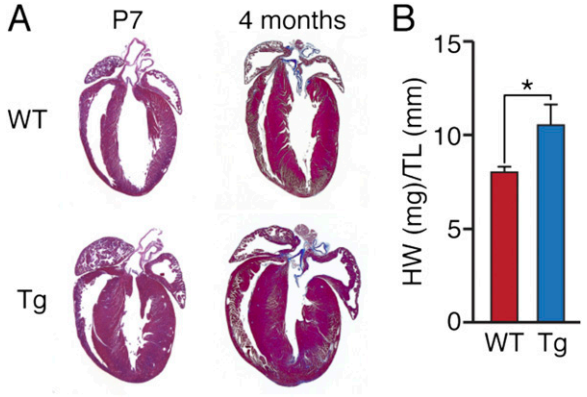

Fig. S4. Yap-S112A overexpression increases heart size in αMHC-Yap-S112A Tg mice. (*A*) Masson's trichrome-stained sections of WT and αMHC-YapS112ATg hearts at age 7 d and 4 mo. (*B*) Measurement of HW:TL ratio indicating increased heart size in αMHC-YapS112ATg mice. Data are mean ± SD. $*P < 0.05$.

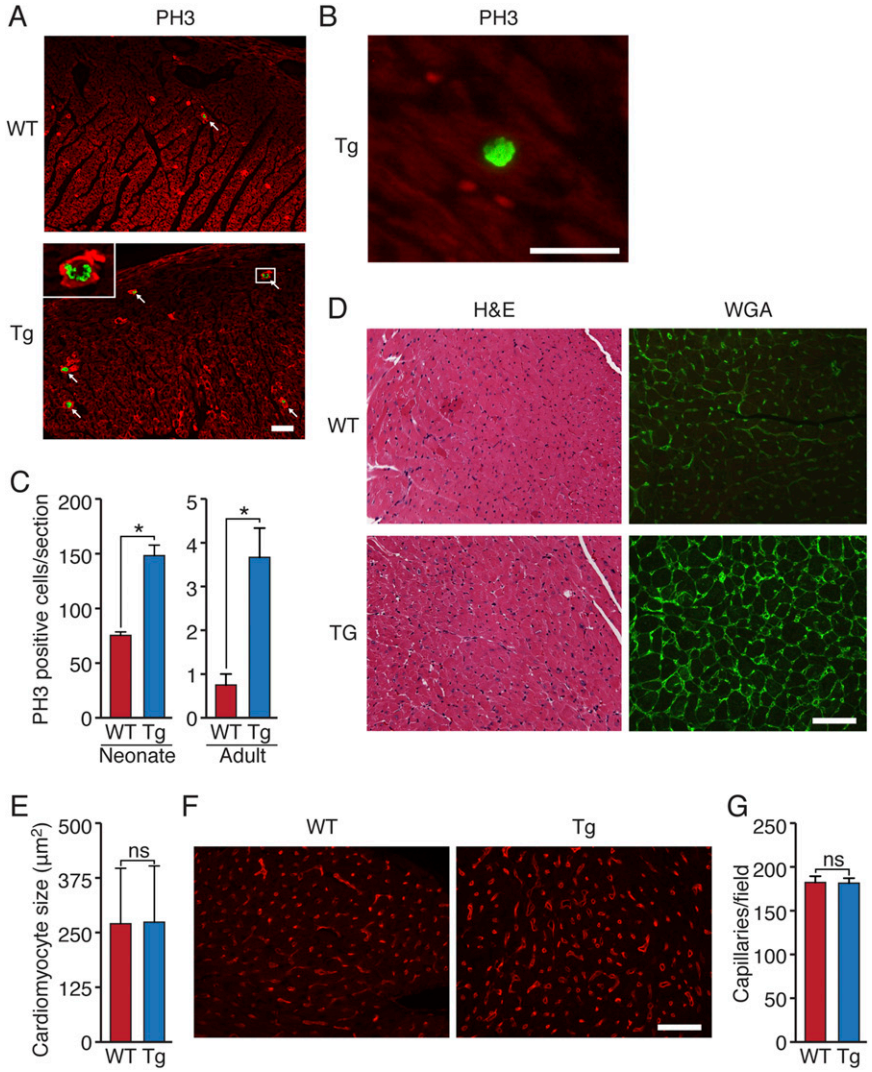

Fig. S5. Yap-S112A overexpression enhances cardiomyocyte proliferation. (*A*) PH3-stained sections of hearts from WT and αMHC-YapS112A Tg mice at P7. The green signal and white arrows indicate PH3-positive staining, and the red signal shows cTnT immunostaining. (Scale bar: 100 μm.) (*B*) PH3-stained sections of hearts from WT and αMHC-YapS112A Tg mice at P28. The green signal and white arrows indicate PH3-positive staining, and the red signal shows cTnT immunostaining. (Scale bar: 100 μm.) (*C*) Quantification of PH3 immunostaining of WT and Tg neonate and adult mouse heart sections. Data are mean ± SD. $*P < 0.05$. (*D*) Wheat germ agglutinin (WGA)-stained sections of the LV compact zone in hearts of WT and αMHC-YapS112A Tg mice at P28 showing similar cardiomyocyte size in the two genotypes. (Scale bar: 100 μm.) (*E*) Quantification of cardiomyocyte area. $n = 3$. Data are mean ± SD. (*F*) Lectin *Bandeiraea simplicifolia*-stained sections of hearts from WT and αMHC-YapS112A Tg mice at P28. (*G*) Quantification of capillary numbers by immunostaining with lectin. $n = 4$. ns, not statistically significant.

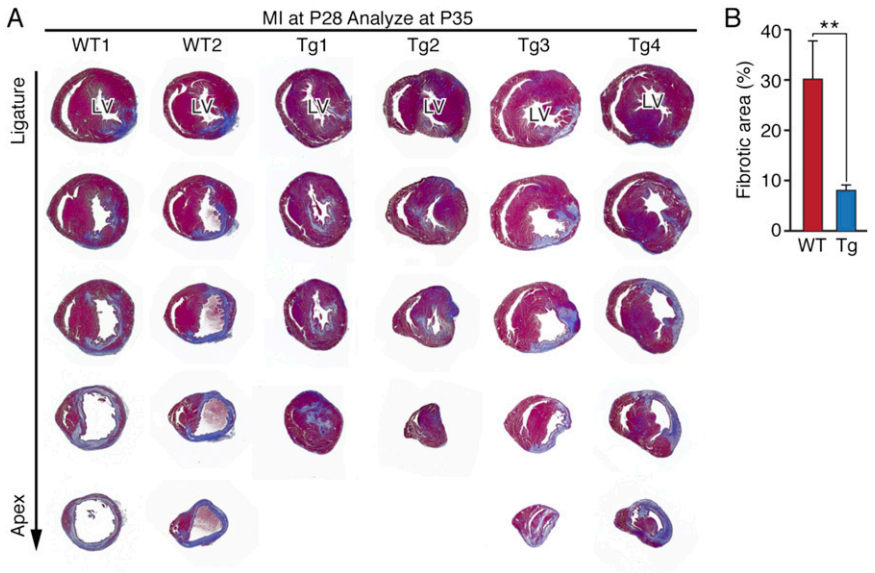

Fig. S6. Activated Yap enhances cardiac regeneration. (*A*) Masson's trichrome-stained heart sections of WT and αMHC-YapS112A Tg mice at 7 d after LAD ligation performed at P28. Serial sections were cut at 500-μm intervals from the site of the ligature toward the apex. (*B*) Quantification of fibrotic areas in heart sections displayed in *A*. $n = 3$ for WT; $n = 4$ for Tg. Data are mean ± SD. $^{**}P < 0.005$.

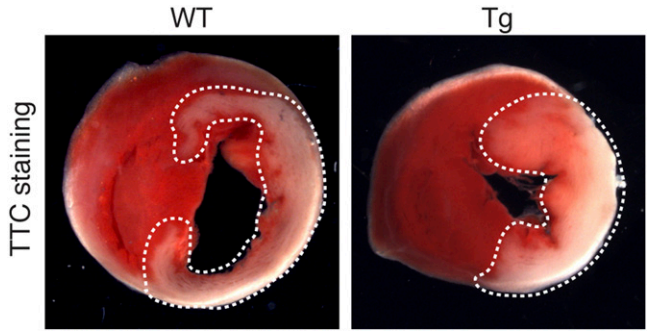

Fig. S7. Myocardial necrosis after LAD ligation. Representative images of WT and αMHC-YapS112A hearts at 3 d after LAD ligation at P28. Staining with the viability indicator TTC revealed similar infarct sizes in WT and Tg hearts. White myocardium represents the infarct area of necrosis.

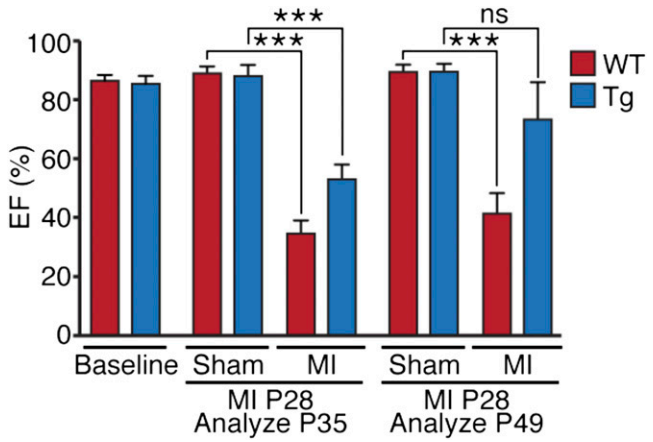

Fig. S8. Activated Yap improves function of ischemic hearts. Cardiac function of WT and αMHC-YapS112A Tg mice subjected to LAD ligation was evaluated by echocardiography at various time points. Ejection fraction (EF) is shown. Data are mean ± SD. $^{***}P < 0.001$. ns, not statistically significant.

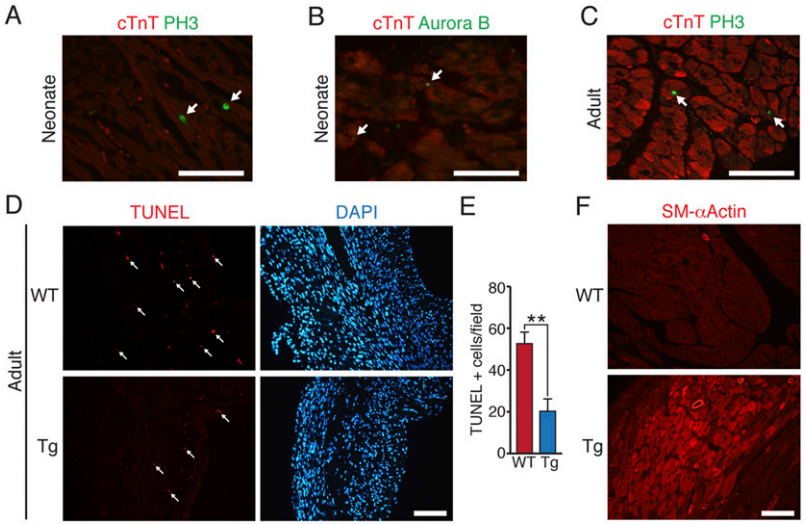

Fig. S9. Yap promotes cardiomyocyte proliferation and improves survival after MI. (*A* and *B*) PH3-stained (*A*) and Aurora B-stained (*B*) sections of αMHC-YapS112A Tg mouse heart at 7 d post-MI performed at P7. (Scale bars: 100 μm.) (*C*) PH3-stained sections of hearts of αMHC-YapS112A Tg 7 d post-MI performed at P28. The green signal and white arrows indicate PH3- positive staining, and the red signal shows cTnT immunostaining. (Scale bar: 100 μm.) (*D*) TUNEL-stained sections of hearts of WT and αMHC-YapS112A Tg mice at 7 d post-MI performed at P28. The red signal and white arrows indicate TUNEL-positive staining. (Scale bar: 200 μm.) (*E*) Quantification of TUNEL-positive cells ($n = 4$). Data are mean ± SD. ** $P < 0.005$. (*F*) Smooth muscle α-actin–stained sections of adult hearts from WT and αMHC-YapS112A Tg mice. (Scale bar: 200 μm.)